Turbulent flux exchange characteristics of air-ice-sea above the Arctic Ocean during the polar day period*

QU Shaohou (曲绍厚), HU Fei (胡 非), BAI Jianhui (白建辉) and LI Yaqiu (李亚秋)

Institute of Atmospheric Physics, State Key Laboratory of Atmospheric Boundary Layer Physics and Atmospheric Chemistry, Chinese Academy of Sciences, Beijing 100029, China

Received November 8, 2000; revised December 28, 2000

Abstract Chinese "Xue Long" breaker made its first voyage to the Arctic Ocean for scientific expedition from July to September, 1999. The tethersonde meteorological tower (TMT) sounding system was used to probe the temperature, humidity, air pressure, wind direction and wind speed on different underlying surfaces above the Arctic Ocean. The probed data were used for calculating the roughness length z_0, momentum flux M, drag coefficient C_{DD}, sensible heat flux H_{SS}, bulk transfer coefficient C_{HH} for sensible heat, latent heat flux H_{LL}, and bulk transfer coefficient C_{EE} for latent heat of air-ice-sea on different underlying surfaces. They vary within the ranges of (0.2 ~ 1.0) mm, (1.14 ~ 9.19) × 10^{-2} N/m^2, (0.87 ~ 1.76) × 10^{-3}, −(4.2 ~ 12.5) W/m^2, (0.84 ~ 1.37) × 10^{-3}, −6.6 ~ 23.6 W/m^2 and (0.85 ~ 1.40) × 10^{-3}, respectively. It shows that the drag coefficient is greater than the latent heat transfer coefficient, and again the latent heat transfer coefficient is larger than the sensible heat transfer coefficient. Besides, the fluxes of momentum, sensible and latent heat are apparently correlated to the mean wind speed and the mean potential temperature difference and mean specific humidity difference.

Keywords: the Arctic Ocean, air-ice-sea exchange, turbulent flux.

As one significant part of the earth climate and environment system (including atmosphere, lithosphere, hydrosphere, biosphere and cryosphere), the Arctic area gives a sensitive response and strong feedback to the global change in environment and climate. Hence, it is one of the most sensitive and crucial areas for the global change in climate and environment. Owing to the unique special geographical position, complicated underlying surfaces, severe climatic and environmental conditions, the fundamental observational data, especially those for air-ice-sea exchange and atmospheric boundary layer (ABL) structure are extremely scarce. It was not until the 1990's that people got to notice the following problems in the arctic climate system: (i) the large discrepancies[1~4] between simulations of global climate models (GCMs) for present or future climate and the observations in the Arctic; (ii) uncertainty[1)] about the impact of the Arctic area on the climate change. These problems arise from an incomplete understanding of the heat balance, vertical exchange and interaction of the turbulent flux of momentum, heat, and substance within the atmosphere-ocean-ice system in different underlying surfaces of the Arctic Ocean.

* Project supported by the National Natural Science Foundation of China (Grant No. 49675252), First CHINARE Expedition of the Chinese Arctic and Antarctic Administration, and Project KZCX2-204 of CAS Knowledge Innovation Program.

1) Moritz, R. E. et al. A research program on the surface heat budget of the Arctic Ocean. Science Plan, 1996.

1 Observational ocean areas and instruments

Figure 1 shows the navigation route of "Xue Long" breaker for its first voyage to the Arctic Ocean from July to September, 1999. The furthest point to the north it reached was 77°30′N, 160°49′W. The tethersonde meteorological tower (TMT) sounding systems were set up in the following ocean areas: ① open sea with 20% ~ 30% floating ice, ② floe sea area with 30% ~ 40% floating ice, ③ floe sea area with 60% ~ 70% floating ice, ④ area with annual large floe ice of 1 km^2, and ⑤ area with perennial large floating ice of 0.3 km^2 (Figure 1).

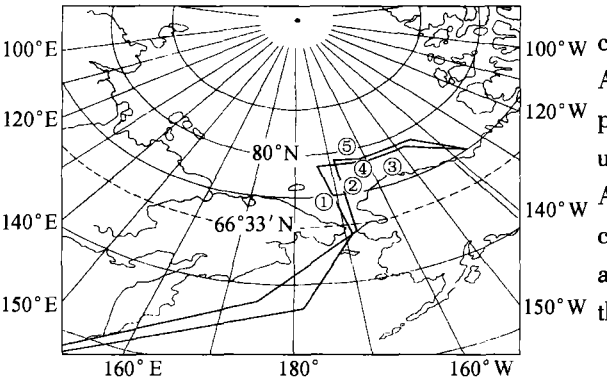

Fig. 1 Navigation route of "Xue Long" breaker (solid line) and the locations of the TMT station: ① 69°59′N, 172°19′W; ② 71°42′N, 168°51′W; ③ 72°24′N, 153°36′W; ④ 73°26′N, 164°59′W; ⑤ 75°02′N, 160°51′W.

Basically the above-mentioned five areas can represent typical characteristics of the Arctic Ocean underlying surfaces during the polar day period, though the portions of those underlying surfaces vary with season or month. As a result, the observed transferring characteristics of the turbulent flux were assumed to be typical of this ocean area during the polar day period.

The TMT sounding system consists of a blimp-shipped balloon, the tethersonde, a receiver, and real-time data processing system. The main specifications of the TMT for atmospheric elements are given in Table 1.

Table 1 Specifications of TMT for atmospheric elements

Element	Range	Telemeric accuracy	Resolution
Temperature/℃	-40 ~ 50	±0.5	0.1
Humidity/RH%	0 ~ 100	±3	0.1
Pressure/hPa	600 ~ 1050	±0.5	0.1
Wind speed/ms^{-1}	0 ~ 20	±0.5	0.2
Wind direction/(°)	0 ~ 360	±5	2

This system can be set up to carry out 6 level gradient observations of atmospheric elements, the distance between the levels can be adjusted according to practical need. When the profile of the atmospheric boundary layer is measured, its special resolution is around 2 m (dependent on the ascending speed of the winch), which is enough for studying the special structure of the atmospheric boundary layer and air-ice-sea interaction. The observations were performed repetitively and constantly with one sensor in the low atmosphere for a total of 70 minutes. The most observations for each layer lasted for 15 s due to the short delay time of the sensor (less than 1 s). The results are the average of measured profiles in many observations.

2 Calculating method

In an atmospheric surface layer of neutral stability, the profiles of velocity $u(z)$, potential temperature $\theta(z)$, and specific humidity $q(z)$ can be expressed in the following semi-logarithmic forms[5]:

$$\frac{u(z)}{u_*} = k^{-1}\ln\left(\frac{z}{z_0}\right), \tag{1}$$

$$\frac{\theta(z) - \theta_0}{\theta_*} = (\alpha_H k)^{-1}\ln\left(\frac{z}{z_\theta}\right), \tag{2}$$

$$\frac{q(z) - q_0}{q_*} = (\alpha_E k)^{-1}\ln\left(\frac{z}{z_q}\right), \tag{3}$$

where z is the height above the surface; k the Von Kàrmàn's constant (0.4); θ_0 and q_0 are the potential temperature and the specific humidity of air on the surface of snow or sea ice or land or water; and $\alpha_H = K_H/K_M$ and $\alpha_E = K_E/K_M$ are the ratios of the scalar turbulent diffusivities K_H and K_E to the turbulent diffusivity for momentum K_M. The relations between the turbulent surface fluxes of momentum M and sensible heat H_S and latent heat H_L; and friction velocity u_*, the potential temperature scale θ_* and the characteristic specific humidity q_* are:

$$M = -\rho u_*^2, \tag{4}$$

$$H_S = -\rho c_p u_* \theta_*, \tag{5}$$

$$H_L = -\rho L u_* q_*, \tag{6}$$

where ρ is the air density, which is a function of air temperature and air pressure; $c_p = 1.0051 \times 10^3$ $J \cdot kg^{-1} \cdot k^{-1}$, the specific heat of air at constant pressure; $L_V = (597 - 0.56T_s) \times 4186.8$ $J \cdot kg^{-1}$, the latent heat of evaporation over water and $L_S = 677.12 \times 4186.8$ $J \cdot kg^{-1}$, the latent heat of sublimation over ice and snow; z_0, z_θ and z_q are the roughness lengths for wind speed, temperature and water vapor, respectively.

The bulk aerodynamic transfer formulae for M, H_S and H_L at the height of 10 m can be written as

$$M = \rho C_D U_{10}^2, \tag{7}$$

$$H_S = \rho c_p C_H U_{10}(\theta_0 - \theta_{10}), \tag{8}$$

$$H_L = \rho L C_E U_{10}(q_0 - q_{10}), \tag{9}$$

where average values of wind speed U_{10}, potential temperature θ_{10} and specific humidity q_{10} are taken from measurements; and C_D, C_H and C_E are the bulk-aerodynamic transfer coefficients for

momentum, sensible heat and latent heat at neutral stability. For neutral stability, from Eqs. (1) ~ (9), the relations between these coefficients and the roughness lengths are respectively:

$$C_D = \frac{k^2}{[\ln(10/z_0)]^2}, \tag{10}$$

$$C_H = \frac{\alpha_H k C_D^{1/2}}{kC_D^{-1/2} - \ln(z_\theta/z_0)}, \tag{11}$$

$$C_E = \frac{\alpha_E k C_D^{1/2}}{kC_D^{-1/2} - \ln(z_q/z_0)}. \tag{12}$$

Hence knowing the roughness lengths and giving z_0, z_θ/z_0, and z_q/z_0; C_D, C_H, and C_E can be obtained from Eqs. (10) ~ (12). Based on the observational results of U, θ and q; M, H_S and H_L at neutral stability can be calculated from Eqs. (7) ~ (9). Parameter z_0 is calculated according to the mean profile method[6]; θ_0 and q_0 which is the saturated specific humidity under sea surface temperature can be obtained by optimal numerical fitting of the TMT observational data and θ_0 can be also measured by an infrared radiometer directly. At the same time, z_θ/z_0 and z_q/z_0 can be obtained by the empirical formula given by Andreas[5]:

$$\ln\left(\frac{z_s}{z_0}\right) = b_0 + b_1 \ln R_* + b_2 (\ln R_*)^2, \tag{13}$$

where $R_* = u_* z/\upsilon$ is the roughness Reynolds number, here $u_* = (\tau/\rho)^{1/2}$; and υ, the kinetic viscosity of air. The values of the coefficients of Eq. (13) are shown in Table 2.

Table 2 Values[5] of the coefficients in Eq. (13), for potential temperature ($z_s = z_\theta$) and for water vapor ($z_s = z_q$)

Coefficient		$R_* \leqslant 0.135$	$0.135 < R_* < 2.5$	$2.5 \leqslant R_* \leqslant 1000$
Potential temperature	b_0	1.250	0.149	0.317
	b_1	0.000	-0.550	-0.365
	b_2	0.000	0.000	-0.183
Water vapor	b_0	1.610	0.351	0.396
	b_1	0.000	-0.628	-0.512
	b_2	0.000	0.000	-0.180

C_{DD}, C_{HH} and C_{EE} for stable and unstable atmosphere are given by[7]

$$\frac{C_{DD}}{C_D} \approx \frac{C_{HH}}{C_H} \approx \frac{C_{EE}}{C_E} \approx 0.1 + 0.03S + 0.9\exp(4.8S) \tag{14}$$

and

$$\frac{C_{DD}}{C_D} \approx 1.0 + 0.47S^{0.5},$$

$$\frac{C_{HH}}{C_H} \approx \frac{C_{EE}}{C_E} \approx 1.0 + 0.63S^{0.5}, \tag{15}$$

in which the parameters for atmospheric stability S and S_0 are

$$S = S_0 \frac{|S_0|}{|S_0| + 0.01},$$

$$S_0 = \frac{T_s - T_a}{U^2[1.0 + \lg(10/z)]^2}. \tag{16}$$

The actual calculating procedure is as follows.

The roughness length z_0, friction velocity u_*, mean wind speed $\bar{U}_0$ at 10 m; and the mean potential temperature difference $\Delta\theta$ and mean specific humidity difference Δq between the surface and the height of 10 m are given by observation. Then we may obtain the drag coefficient C_D, sensible transfer coefficient C_H and latent heat transfer coefficient C_E by Eqs. (10) ~ (12) for a neutral atmosphere, the stability parameter S by Eq. (16), and those for a stable atmosphere by Eq. (15). Finally, we obtain the momentum flux M, sensible heat flux H_{SS} and latent heat flux H_{LL} by Eqs. (7) ~ (9) respectively.

3 Results and conclusions

3.1 Roughness length

In different areas of the Arctic Ocean the roughness lengths are different due to the differences in constituent components and the degree of undulation of underlying surfaces. The largest roughness length is 1 mm for the open sea with 20% ~ 30% floating ice due to the sea surface undulation caused by wind. However, it is less than that at the western tropical Pacific Ocean (about 5 mm) because the wind wave at the Arctic Ocean is suppressed by the sea ice. The roughness length of about 0.4 mm for the areas with 60% ~ 70% floating ice is less than that for those areas with 30% ~ 40% floating ice (about 0.6 mm) as the floating ice is strongly suppressed by the wind wave. The roughness length of 0.3 mm for the perennial ice disk of middle size 0.3 km^2 is larger than that of 0.2 mm for annual ice disk of middle size 1.0 km^2 because the undulation of underlying surface of the former is larger than that of the latter. And the range of roughness length in this area is 0.2 ~ 1.0 mm, which is basically in accord with the range of roughness 0.2 ~ 0.5 mm for the Greenland ice sheet in the melting season[8], and is one order of magnitude larger than that of ice sheet 0.028 mm[9] around the Zhongshan Station in the Antarctica.

3.2 Correlative relation between bulk transfer coefficient and stability parameters

The atmospheric boundary layer of the Arctic Ocean is always in a stable stratification throughout the year[2]. It is necessary to adopt the drag coefficient C_{DD}, sensible heat transfer coefficient C_{HH} and latent heat transfer coefficient C_{EE} for the stratification atmosphere, while using the bulk aerodynamic Formulae (7) ~ (9) to calculate the momentum, sensible and latent heat fluxes. In the previous calculation, the adoption of coefficients of the neutral atmosphere led to an error of 10% ~ 20%, or sometimes even as high as 40% in turbulent fluxes. Fig. 2(a) shows the correlation between turbulent transfer coefficients C_{DD}, C_{HH} and C_{EE} of the stratification atmosphere and their

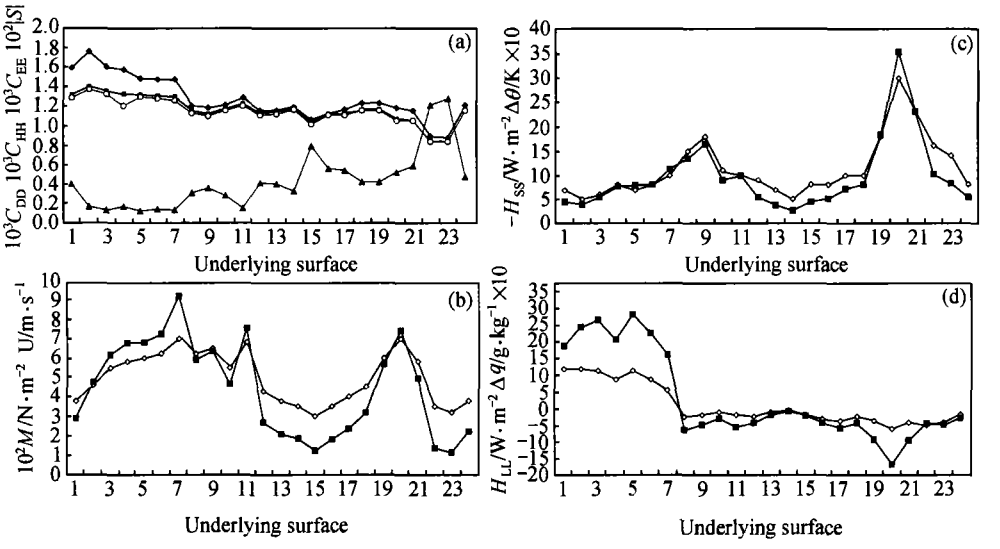

Fig. 2 Variations of parameters on different underlying surfaces at the Arctic Ocean of: (a) C_{DD}(◆), C_{EE}(■) and C_{HH}(◇) and their correlations with the stability parameter $|S|$(▲); (b) momentum flux $10^2 M$ (■) and its correlation with the mean wind speed U(◇); (c) sensible heat flux H_{SS}(■) and its correlation with the difference in mean potential temperature $\Delta\theta$(◇); (d) latent heat flux H_{LL}(■) and its correlation with the difference in mean specific humidity Δq(◇). And the x-axis indicates the underlying surfaces with open sea with 20% ~ 30% floating ice (1 ~ 2), floe sea area with 30% ~ 40% floating ice (3 ~ 4), floe sea area with 60% ~ 70% floating ice (5 ~ 7), area with annual large floating ice (8 ~ 14), and area with perennial large floating ice (15 ~ 24).

stability parameters ($10^2|S|$) for different underlying surfaces. We find in Fig. 2(a) that both are inversely correlated: the more stable the atmosphere, the smaller C_{DD}, C_{HH} and C_{EE}. When $10^2|S|$ is 12.7, $10^3 C_{DD}$, $10^3 C_{HH}$ and $10^3 C_{EE}$ are 0.87, 0.84 and 0.85, respectively. In contrast, when $10^2|S|$ becomes 1.7; $10^3 C_{DD}$, $10^3 C_{HH}$ and $10^3 C_{EE}$ are 1.76, 1.37 and 1.40, correspondingly. In addition, the turbulent transfer coefficients are also dependent on the roughness length. With the same stability parameter, the turbulent transfer coefficient increases with the increasing roughness length. However, the turbulent transfer coefficients are more sensitive to stability than to roughness length. Besides, we know that the turbulent transfer coefficients are proportional to the wind speed under the neutral condition[10].

As is evident in Fig. 2(a), the drag coefficient C_{DD} is larger than the latent heat transfer coefficient C_{EE}, and again C_{EE} is larger than the sensible heat transfer coefficient C_{HH} with the same stability parameter and the same roughness length. The ranges of C_{DD}, C_{HH} and C_{EE} are $(0.87 \sim 1.76) \times 10^{-3}$, $(0.84 \sim 1.37) \times 10^{-3}$, and $(0.85 \sim 1.40) \times 10^{-3}$, respectively.

3.3 Momentum flux and mean wind speed

The momentum flux represents the force of atmosphere exerted on a unit ground area, which is one of the major parts of studying earth-atmosphere interaction. Sea wave, ocean current, swell and storm surge, etc. are the direct responses of ocean to the atmospheric momentum flux transfer. In the

polar area, the transferring characteristics of the atmospheric momentum directly affect the range and thickness of the sea ice and the variation of the ice sheet. Since the momentum flux is proportional to the drag coefficient and to the square of wind speed, while drag coefficient obviously depends on both the stability and roughness length of underlying surface (see Figs. 2(b) and (10)), the momentum flux is dependent on both dynamic and thermodynamic processes as well as the features of underlying surface. Sensitivity experiments show that the momentum flux transferred from the atmosphere to the ground surface is most sensitive to the wind speed, and also to a lesser degree sensitive to stability and roughness length. Fig. 2(b) shows that the momentum flux transferred from atmosphere to ocean (or ice) in that area exhibits an evident positive correlation with the mean wind speed. The calculating results show that for drag coefficient C_{DD} in the range of $(0.87 \sim 1.76) \times 10^{-3}$ and the mean wind speed in the range of $(3.0 \sim 7.0)$ m/s during the polar day period of this sea area, the variation range of the momentum flux transferred from the atmosphere to the ocean is $(11.4 \sim 91.9) \times 10^{-3}$ N/m^2, which is much larger than that of the atmosphere to the ice sheet on the Antarctic continent[9]. The phenomenon is attributed to the fact that the roughness length of the sea surface in this area is much larger than that of the ice sheet in the Antarctica. And it is nearly equivalent to that during a severe convective weather process in the western tropical Pacific Ocean[11] and much less than that during the westerly wind burst over the western tropical Pacific Ocean[12].

3.4 Sensible heat flux and the difference in mean potential temperature

The different features of underlying surfaces and the sustained existence[1)] of atmospheric inversion layers in the Arctic Ocean lead to the complicated transferring characteristics of the sensible and latent heat flux between air-ice-sea, thus affecting the range and thickness of the sea ice.

Figure 2(c) presents the relation between the sensible heat flux and the difference in mean potential temperature in different underlying surfaces above that area. It shows that whatever in the open sea, the area with 30% ~ 40% or 60% ~ 70% floating ice, and annual and perennial ice disks of middle size, during not only the polar night period but also the polar day period, the heat in the atmosphere is transferred to sea or floating ice in the form of sensible heat due to the existence of a sustaining inversion layer (except for some individual moment for a clear day). On average, the heat transferred is about -4.2 W·m^{-2} in the open sea, -6.5 W·m^{-2} for the area with 30% ~ 40% floating ice, about -9.1 W·m^{-2} for the area with 60% ~ 70% floating ice, about -8.7 W·m^{-2} and -12.5 W·m^{-2} for annual and perennial ice disks of middle size (minus means atmosphere is the heat source), respectively. With an apparent correlation between $|H_{SS}|$ and $|\Delta\theta|$ (Fig. 2(c)), the sensible heat flux is mainly dependent on the mean potential temperature difference between observational heights, the sensible transfer coefficient and the wind speed.

3.5 Latent heat flux and the difference in mean specific humidity

Figure 2(d) presents the latent heat flux with respect to the difference in the mean specific humidity at different underlying surfaces during the polar day period in that area. Fig. 2(d) shows

1) Qu S. H. et al. Characteristics of ABL structure over the Arctic Ocean and adjacent sea during polar day periods. J. Geophys. Res., (accepted).

that the latent heat flux is positive for the area of the open sea with 20% ~ 30% or with 30% ~ 40% or 60% ~ 70% floating ice, namely the heat is transported from sea to atmosphere. The main reason is that the underlying surface has the ocean portion, the albedo of which is small, about 0.1 ~ 0.2. The solar radiation absorbed by the ocean transfers to the atmosphere in the form of latent heat. On the other hand, the latent heat flux is negative for annual or perennial ice disk with middle size (Fig. 2(d)), namely, the water vapor is transported from atmosphere over the ice disk to ice. This is due to humidity inversion by advection from the adjacent water vapor over the open sea or floating ice area to the atmosphere over ice disk of 1.0 km^2 and 0.3 km^2. In addition, we find that the latent heat fluxes for open sea with 20% ~ 30%, for the area with 30% ~ 40% and 60% ~ 70% floating ice on average are 21.6 $W \cdot m^{-2}$, 23.6 $W \cdot m^{-2}$ and 22.3 $W \cdot m^{-2}$, respectively. They are almost the same, which is the synthetic results considering both dynamic and thermodynamic processes. However, they become around -3.9 and -6.6 $W \cdot m^{-2}$ for the area of annual and perennial ice disk. The latent heat flux $|H_{LL}|$ is proportional to the difference in mean specific moisture $|\Delta q|$ between measured heights as well as to the latent transfer coefficient and wind speed (Figure 2(d)).

Acknowledgements The authors wish to express their thanks to Dr. Qin Weijia from Chinese Arctic and Antarctic Administration for his help. Thanks are also due to Profs. Bian Lingen, Lu Changgui and Zhou Libo for taking part in the observation.

References

1 Hu, F. Turbulence, Intermittency and Atmospheric Layer (in Chinese). Beijing: Science Press, 1995.
2 Houghton, J. T. et al. Climate Models-evaluation. Climate Change, London: Cambridge University Press, 1995.
3 Kahl, J. D. et al. Absence of evidence for greenhouse warming over the Arctic Ocean in the past 40 years. Nature, 1993, 361: 335.
4 Johannessen, O. M. The Arctic shrinking sea ice. Nature, 1995, 376: 126.
5 Andreas E. L. A theory for the scalar roughness and the scalar transfer coefficients over snow and sea ice. Boundary-Layer Meteorology, 1987, 38: 159.
6 Handorf, D. et al. The stable atmosphere boundary layer over an Antarctic ice sheet. Boundary-Layer Meteorology, 1999, 91: 165.
7 Kondo, J. Air-sea bulk transfer coefficients in diabatic conditions. Boundary-Layer Meteorology, 1975, 9: 91.
8 Meesters, A. G. C. A. et al. Turbulence observations above a smooth melting surface on the Greenland Ice Sheet. Boundary-Layer Meteorology, 1997, 85: 81.
9 Qu S. H. Atmospheric boundary layer structure and turbulent flux transfer over the Zhongshan Station area, Antarctica. Chinese Journal of Polar Science, 1997, 8(2): 79.
10 Greenaert, G. L. On the importance of the drag coefficient in air-sea interaction. Dynamics of Atmosophere and Ocean, 1987, 11: 19.
11 Qu S. H. Characteristics of turbulent fluxes in the strong convective weather process over the western tropical Pacific Ocean. Plateau Meteorology (in Chinese), 1994, 13(1): 75.
12 Qu S. H. Characteristics of turbulent fluxes during westerly wind burst at the western tropical Pacific Ocean. J. Atmospheric Sciences (in Chinese), 1996, 20(2): 188.